



Utilizing a New Voltage Stability Index in Distribution Power System in Presence of Wind Turbine Units

A. H. Foomani, M. Moradlou*, P. Nazarian

Department of Electrical Engineering, Zanjan Branch, Islamic Azad University, Zanjan, Iran

PAPER INFO

Paper history:

Received 12 August 2023

Received in revised form 08 October 2023

Accepted 02 November 2023

Keywords:

Voltage Stability Index

Analytical Hierarchy Process

Active Distribution Network

Multi-criteria Decision Formation

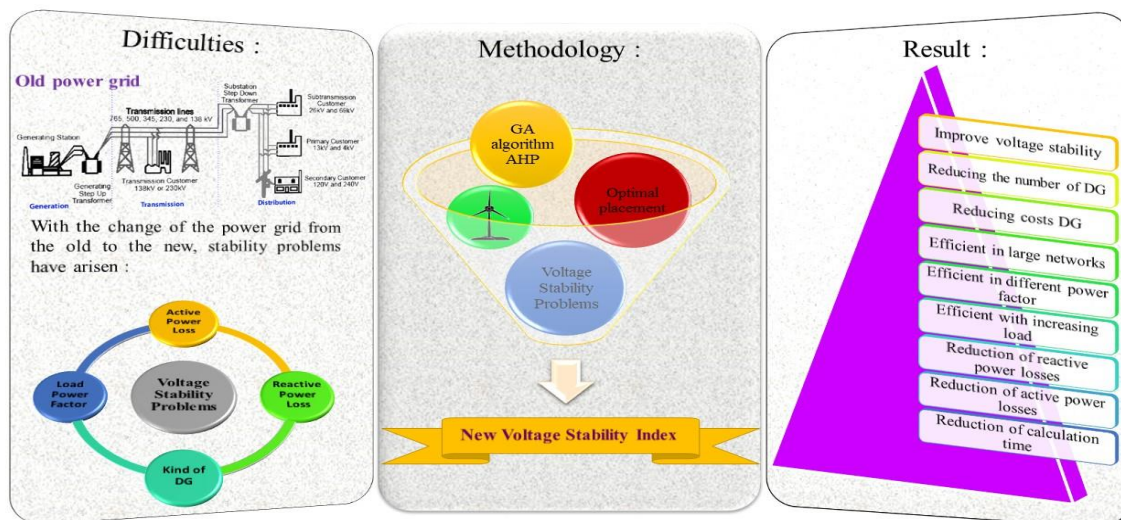
Wind Turbine

ABSTRACT

Equipping renewable energy resources generation units in the distribution network to reduce economical and emission concerns are the examples of active distribution network (ADN). The other advantages of utilizing distributed generators (DGs) are improving technical constraints of ADN. In this paper multi-benefit functions are defined as main functions. Each of functions illustrates the positive impacts of utilizing wind turbines in the improving technical constraints of the ADN. Voltage stability (VS) is one of the main technical indices of the ADN. Several VSIs are defined to evaluate voltage stability of the ADN. The previous indices could not give the proper results about allocating DGs and accurate evaluating of voltage stability of ADN. This work proposes the new VSI. To this aim active power loss (APL), reactive power loss (RPL) and voltage stability index (VSI) are considered as technical constraints. In order to evaluate the presence of WT on improving APL and RPL, WTs are considered in two operational modes; unified power factor (UPF) and (APF). The main benefit function is solved by implementing genetic algorithm (GA). Multiplying weights to the APL, RPL and VSI (which are improved by attendance WTs) in benefit function formulation, make the multi-criteria decision formation to the proposed optimization problem. By employing analytical hierarchy process (AHP) technique and considering each technical constraints as main criteria, the obtained solutions are arranged. To verify the positive effectiveness of the proposed VSI, its results are compared with the results of other VSIs in the 33, 67 and 118 bus IEEE radial DN.

doi: 10.5829/ije.2024.37.04a.11

Graphical Abstract



*Corresponding Author Email: majid.moradloo@iauz.ac.ir (M. Moradlou)

NOMENCLATURE		
Index		
t	Time in second	Pi
i	The counter for the number of WT units	Qi
Parameters		Intr
τ	Planning horizon (year)	Kqv
ρ	Price of purchasing/selling of power (\$)	α
Vcut-in	The lower bound operational velocity of WT (m/s)	$DLF_{i,t,h}^S$
Vcut-out	The upper bound operational velocity of WT (m/s)	K_{pv}
Vrated	Nominal velocity of WT (m/s)	Kqv
T	Planning horizon (hour)	Function
PrWT	Rated power of WT (kW)	VPI
ICWT	The total capital cost of WT	RPLI
OCWT	The total operational cost of WT	VSI
LP	Purchased power from an upstream network	APL
LS	Sold power from upstream network	DNO
IWT	Current of WT	DSM1
Infr	Inflation rate (%)	DSM2
		DSM3
		DSM4

1. INTRODUCTION

Due to the lack of fossil fuels and their environmental issues, such as global warming and pollution, energy administrators think of using alternative cheap, available, and clean energy resources. The wind is one of the clean and available resources. By integrating wind turbines (WT), the necessity to install a new central (fossil fuel) power plants is diminished. WT operates in both grid-connected and isolated conditions. Recently equipping distribution networks with WT to improve system technical constraints is the main aim of researchers. The role of WT in improving several technical constraints of distribution network (DN), such as: reliability, voltage stability, active and reactive power loss reduction, are considered in the recent kind of literature. By connecting DGs in the proper buses of DN, besides improving the voltage profile of buses, total active and reactive losses are reduced (1). Optimal integration of distributed generators (DGs), improved the voltage stability of buses (2). Mobashsher et al. (3), introduced an optimal voltage control (OVC) framework for islanded microgrids (MGs) as a unified hierarchical control scheme. Investing in private enterprises in the energy section by installing WTs in the DN was studied by Tooryan et al. (4). Energy not supplied with considering reliability indices in the planning horizon is the primary function as introduced by Yousefipour et al. (5). Integrating WTs and energy storage systems (ESS) to optimal managing of generation and demand by considering WT probabilistic behavior was studied by Wang et al. (6). Elmaadawy et al. (7) studied impacts of utilizing WT on improving voltage stability and reducing active power loss in the 13 and 69

buses, IEEE system. Non-optimal power flow could be caused by the voltage drops and blackouts due to voltage instability of DN (8). An economic dispatch of generation units to calculate the cost of DG installation and system technical constraints is called power flow (9). The destructive effects of installing WT in the DN are; voltage rise and fluctuation stability and increasing short circuit capacity level (10). Presenting the voltage stability index to optimal siting and sizing of DGs are the main aims of the recent kind of literature (11). Azad et al. (12) proposed both of VSI and APLI as primary function of planning problem. Mirjalili et al. (13) also proposed the new indices to improve voltage stability margin (VSM) for both of active and reactive power at the weakest bus after installing WTs. The output power of wind turbines has been injected into the 30 bus system in the South Sulawesi network in order to improve the stability of the network voltage (14). The multi objective performance index (MOPI) is introduced to optimal siting and sizing of DG in the DN. By implementing weighted coefficient, many technical constraints are combined and solved under various operating circumstance (15). Nafeh et al. (16) studied changing parking lot (PL) to the intelligent parking lot (IPL) with installing WT. Onlam et al. (17) obtained the best allocation buses of WTs, the power stability index (PSI) which was proposed with considering 2-bus system with less than the unity margin for a voltage stable operation. Voltage deviation index (VDI) is presented as an absolute value of bus voltage deviation than the unity margin (18). To estimate voltage drop in a power system, voltage collapse prediction index (VCPI) is defined based on the system variables such as the bus voltage magnitude, buses voltage angle, and

admittance matrix of system (19). Hassani et al. (20) introduced the new system sensitivity analyze index (SAI) to measure active and reactive power in the weak buses. To identify the weak bus of radial DN, the bus participation factor (BPF) was proposed by Guerrero et al. (21). Sundarajoo and Soomro (22) proposed an optimal method of load shedding under voltage (UVLS) to optimally predict the amount of shed load and the best place for load shedding. In this work, the stability index (SI) and feed forward back propagation neural network (FFBPNN) are adopted to prevent voltage collapse and blackout by reducing voltage instability following the addition of load in the distribution system. However, in this simulation, the old voltage stability index is still used. Variations in the power factor of different loads as well as the presence of distributed generation have not been investigated in it. Sadeghi and Akbari Foroud(23) considered line length effects on the voltage stability by introducing the new VSI. This index could asses the voltage stability of transmission and distribution network separately and together. Effects of tapchanger and distributed generators on voltage stability of distribution network is analyzed by presenting the new VSI (24).

As it is reviewed from the last literatures, due to importance of technical constraints, authors considered several technical criteria in works. There are different VSIs which were introduced. The presented VSI in the latest researches includes the voltage deviation from the 1 p.u. Therefore, these indices could not give the proper results about allocating DGs and accurate evaluating of voltage stability of DN. In this paper impacts of considering WT in both modes: unity power factor (PF) and adjusted PF on improving technical constraints as: voltage stability (VS), voltage profile and technical constraints such as reactive power loss and active power loss was studied. Figure 1 depicts the concept of main aims of this paper .

The main contributions of this paper are listed as follows:

- Introducing the new voltage stability index
- Optimal siting and sizing of DGs in unified and adjustable power factor
- Applying Analytical Hierarchy Process (AHP) to solve multi-ceria decision problem
- Considering several kinds of loads (residential, industrial and commercial)

The other parts of paper are organized as follows:

In the section 2, problem definition and optimization algorithm has been discussed in details. In section 3, all of obtained results in the different scenarios have been demonstrated. Discussion and conclusion are described respectively in sections 4 and 5.

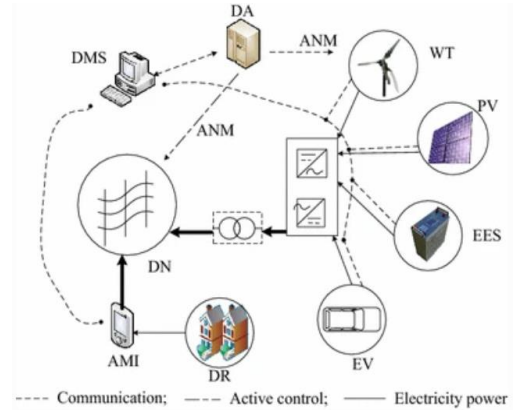


Figure 1. Optimal siting and sizing of DGs

2. PROBLEM DEFINITION

In this paper impacts of optimal siting and sizing of DGs on improving voltage stability, active power loss, line flow limitation, reactive power loss and voltage profile index has been studied. Each of indices are defined as follows:

$$DSM_1 = \max \left\{ B_{Total}^{disch\ arg\ e} + B_{Total}^{Load} + B_{Total}^{Loss} + B_{Total}^{WT} - C_{Total}^{inv} \right\} \quad (1)$$

$$DSM_2 = \max \left\{ B_{Total}^{disch\ arg\ e} + B_{Total}^{Load} + B_{Total}^{VSI} + B_{Total}^{WT} - C_{Total}^{inv} \right\} \quad (2)$$

$$DSM_3 = \max \left\{ B_{Total}^{disch\ arg\ e} + B_{Total}^{Load} + B_{Total}^{LFL} + B_{Total}^{WT} - C_{Total}^{inv} \right\} \quad (3)$$

$$DSM_4 = \max \{ W_1 \times DSM_1 + W_2 \times DSM_2 + W_3 \times DSM_3 \} \quad (4)$$

Amounts of archived benefits by installing WT is calculated as follows :

$$B_{Total}^{WT} = \sum_{t=1}^T \sum_{h=1}^{N_h} \sum_{i=1}^{N_b} \sum_{WT=1}^{N_{WT}} (P_{t,h}^{WT} \times \rho_{t,h} \times \tau_{t,h}) \times \left(\frac{1+InfR}{1+IntR} \right)^t \quad (5)$$

The total benefits which are obtained by considering positive impacts of WT are calculated as follows:

$$B_{Total}^{Loss} = \sum_{t=1}^T \sum_{h=1}^{N_h} [(P_{loss,t,h}^{without\ WT} - P_{loss,t,h}^{with\ WT}) \times \rho_{t,h} \times \tau_{t,h}] \times \left(\frac{1+InfR}{1+IntR} \right)^t \quad (6)$$

Amounts of total achieved benefits by reducing the amount of purchased/sold energy from upstream grid is determined as follows:

$$C_{Total}^{Load} = \sum_{t=1}^T \sum_{h=1}^{N_h} (P_{t,h}^{grid} \times \rho_{t,h}^{grid} \times \tau_{t,h}^{grid}) \times \left(\frac{1+InfR}{1+IntR} \right)^t \quad (7)$$

$$R_{Total}^{Load} = \sum_{t=1}^T \sum_{h=1}^{N_h} (P_{t,h}^{Load} \times \rho_{t,h}^{Load} \times \tau_{t,h}^{Load}) \times \left(\frac{1+InfR}{1+IntR} \right)^t \quad (8)$$

$$B_{Total} = R_{Total}^{Load} - C_{Total}^{Load} \quad (9)$$

$$P_{t,h}^{grid} = \begin{cases} P_{t,h}^{Load} + P_{Loss} + P_{charge}^b - P_{WT} \\ P_{t,h}^{Load} + P_{Loss} - P_{discharge}^b - P_{WT} \end{cases} \quad (10)$$

2. 1. Active Power Loss (APL) Connecting DG's to the buses, reduce the amount of active power loss. In this section to evaluate DG's role in the reduction of active power loss, the related index is defined as follows (25):

$$APLI = \frac{APL_{Old} - APL_{New}}{APL_{Old}} \quad (11)$$

where :

$$APL_{Old} = \sum R_i \times I_i^2 \quad (12)$$

2. 2. Rective Power Loss (RPL) Connecting DG's to the distribution system buses, reduce the amount of reactive power loss, by modifying the value of the buses voltage. The index to evaluate the value of DG's positive impacts in reducing reactive power loss is defined as follows (25):

$$RPL = \frac{RPL_{Old} - RPL_{New}}{RPL_{Old}} \quad (13)$$

Where :

$$RPL_{Old} = \sum X_i \times I_i^2 \quad (14)$$

2. 3. Line Flow Limitation (LFL) In this section the new voltage stability index and path of achieving its mathematical model is described. Figure 2 shows the distribution system with both of sending and receiving (feeder and load) parts. Branch current and voltage of receiver section are received by equations (14-17):

$$LFL = \text{Max} \left(\frac{S_{ij}}{CS_{ij}} \right) \quad (15)$$

2. 4. New voltage stability index (VSI) To avoid occurring overload in the branches, considering the allowable limit of load flow is important. To evaluate the impacts of connecting DG's on the line's load flow, the line flow limit index is defined as FOLLOWS (26):

$$I_{12} = \left[\frac{P_2 + jQ_2}{V_2 \angle \delta} \right]^* \quad (16)$$

$$V_2 \angle \delta = V_1 \angle 0 - (R + jX) I_{12} \quad (17)$$

$$V_2 \angle \delta = V_1 \angle 0 - (R + jX) \left[\frac{P_2 + jQ_2}{V_2 \angle \delta} \right]^* \quad (18)$$

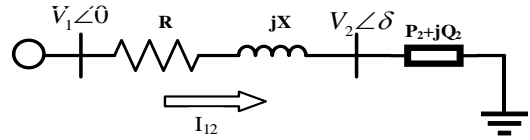


Figure 2. Radial distribution system

$$V_2 \angle \delta = V_1 \angle 0 - (R + jX) \left[\frac{P_2 - jQ_2}{V_2 \angle \delta} \right]^* \quad (19)$$

By multiplying two sides of Equation 19 in $V_2 \angle -\delta$, it will have:

$$V_2^2 = V_1 V_2 \angle -\delta - (R + jX)(P_2 - jQ_2) \quad (20)$$

With rewriting phrase $V_1 V_2 \angle -\delta$ in complex form, the below equations have been found:

$$V_2^2 = V_1 V_2 \cos \delta - jV_1 V_2 \sin \delta - (R + jX)(P_2 - jQ_2) \quad (21)$$

$$V_2^2 + [P_2 R + Q_2 X + j(P_2 X - Q_2 R)] = V_1 V_2 \cos \delta - jV_1 V_2 \sin \delta \quad (22)$$

With separating the imaginary and real parts, it will be noticed that:

$$V_2^2 = P_2 R + Q_2 X = V_1 V_2 \cos \delta \quad (23)$$

$$(P_2 X - Q_2 R) = -jV_1 V_2 \sin \delta \quad (24)$$

$$R = \frac{P_2 X + V_1 V_2 \sin \delta}{Q_2} \quad (25)$$

With replacing Equation 25 in Equation 23, it will be noticed that:

$$V_2^2 + P_2 \frac{P_2 X + V_1 V_2 \sin \delta}{Q_2} + Q_2 X = V_1 V_2 \quad (26)$$

$$V_2^2 + \left(\frac{P_2 \sin \delta V_1}{Q_2} - V_1 \cos \delta \right) V_2 + \left(\frac{P_2^2}{Q_2} + Q_2 \right) X = 0 \quad (27)$$

It's clear that, buses with stable voltage are received by employing $b^2 - 4ac \geq 0$ as follows:

$$\left(\frac{P_2 \sin \delta V_1}{Q_2} - V_1 \cos \delta \right)^2 - 4 \left(\frac{P_2^2}{Q_2} + Q_2 \right) X \geq 0 \quad (28)$$

$$1 = \frac{4 \left(\frac{P_2^2}{Q_2} + Q_2 \right) X}{\left(\frac{P_2 \sin \delta V_1}{Q_2} - V_1 \cos \delta \right)^2} \quad (29)$$

The new voltage stability index is defined as follows:

$$VSI = \left| 1 - \frac{4 \left(\frac{P_2^2}{Q_2} + Q_2 \right) X}{\left(\frac{P_2 \sin \delta V_1}{Q_2} - V_1 \cos \delta \right)^2} \right| \quad (30)$$

2. 5. Wind Turbine To use wind energy and convert its energy to the electrical energy, WT has been used. Due to probabilistic behavior of wind velocity, the output

power of WT is probabilistic. According to the WT constructions and robustness of WT impeller, lower and upper bond of velocity are defined as V_{cut-in} and $V_{cut-out}$ Its output power is calculated as follows (2):

$$P^{Out-WT} = \begin{cases} 0 & V < V_{cut-in}, V > V_{cut-out} \\ P_{rated} \frac{V - V_{cut-in}}{V_{rated} - V_{cut-in}} & V_{cut-in} < V < V_{rated} \\ P_{rated} & V_{rated} < V < V_{cut-out} \end{cases} \quad (31)$$

2. 6. Load Model In this paper, non-linear voltage dependence load is considered in beside of daily load. Daily load includes three demand levels (low, basic and peak load) (27):

$$P_{i.t.h}^{D.s} = P_i^D \times DLF_{i.t.h}^S \times (1 + \alpha)^t \quad (32)$$

$$Q_{i.t.h}^{D.s} = Q_i^D \times DLF_{i.t.h}^S \times (1 + \alpha)^t \quad (33)$$

$$S_{i.t.h}^{D.s} = P_{i.t.h}^{D.s} + jQ_{i.t.h}^{D.s} \quad (34)$$

Mathematical model of buses active and reactive power voltage dependency is defined as follows (28):

$$P_i = P_{i.t.h}^{D.s} \times \left(\frac{V_i}{V_{oi}}\right)^{k_{pv}} \quad (35)$$

$$Q_i = Q_{i.t.h}^{D.s} \times \left(\frac{V_i}{V_{oi}}\right)^{k_{qv}} \quad (36)$$

2. 7. Power Flow In this section the Newton Raphson-based power flow technique is used to obtain buses voltages and branches current. For each demand level and year of planning horizon, power flow equations are calculated as follows (29):

$$P_{t.h}^{grid} + P_{t.h}^{b} + P_{t.h}^{WT} - P_{t.h}^{De} - V_{i.t.h}^e \sum Y_{ij} V_{i.t.h}^e \times \cos(\delta_{i.t.h}^e - \delta_{i.t.h}^e - Q_{ij}) = 0 \quad (37)$$

$$Q_{t.h}^{grid} - Q_{t.h}^{De} - V_{i.t.h}^e \sum Y_{ij} V_{i.t.h}^e \times \sin(\delta_{i.t.h}^e - \delta_{i.t.h}^e - Q_{ij}) = 0 \quad (38)$$

2. 8. AHP Technique Analytical Hierarchy Process (AHP) is the one of most efficient technique to solve multi-criteria problem. This technique by evaluating the problem in the three steps, solve the issues as follows:

- Describing problem
- Listing the various of solving paths with determining alternatives and attributes of them
- Selecting the optimum criteria of solutions among others

Figure 3 illustrates the flowchart of optimization algorithm. Figure 4 illustrates the stages of AHP. As it is seen, the optimization algorithm includes two steps. In the first steps by utilizing GA, problem is solved and in the second step, by utilizing AHP, the optimum criteria

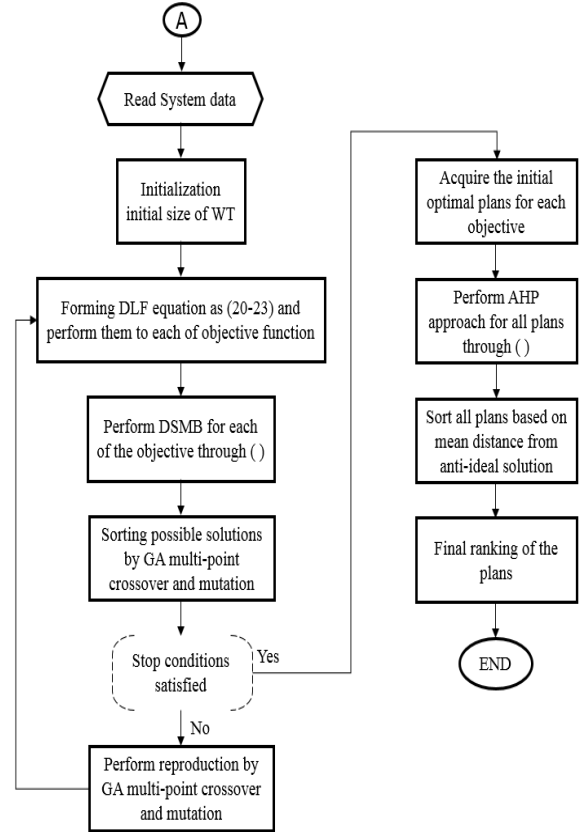


Figure 3. Flowchart of optimization algorithm

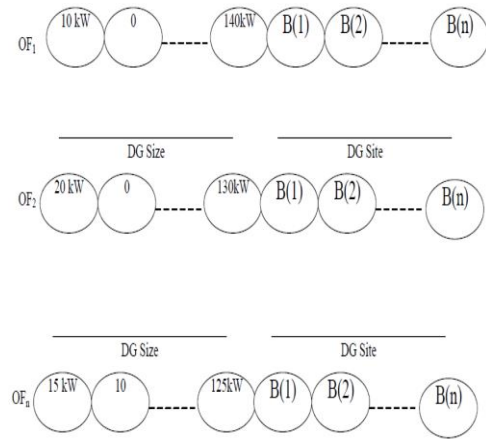


Figure 4. Special chromosome

are selected. Since benefit function is formed by multiplying weights to each technical functions, GA by assigning the larger value to the main technical constraint, start the solving of optimization problem.

2. 9. Optimization Algorithm In this paper, genetic algorithm (GA) and AHP are used to solve optimization algorithm. In the first stage, GA obtained the optimal solutions and in the second stage solutions are arranged

by utilizing AHP. Both of GA and AHP are defined as follows :

In this paper to solve multi-criteria optimization problem, multi objective genetic algorithm (MOGA) is used. The routine GA includes three main steps as follows (30):

- Initializing with coding base chromosome with problem variables
- Crossover
- Mutation

The special chromosome which is codified with the problem variables is illustrated in Figure 4. Crossover and mutation are shown in Figure 5.

All stages of AHP technique are listed as follows:

Formation a(ij) Pair-wise comparison matrix:

$$a_{ij} = \begin{bmatrix} a_{11} & a_{12} & a_{13} & \dots & a_{1n} \\ a_{21} & a_{22} & a_{23} & \dots & a_{2n} \\ \dots & \dots & \dots & \dots & \dots \\ a_{n1} & a_{n2} & a_{n3} & \dots & a_{nn} \end{bmatrix} \quad (39)$$

Modelling normalized matrix as:

$$N_{ij} = \begin{bmatrix} \frac{a_{11}}{\sum_{i=1}^n a_{i1}} & \frac{a_{12}}{\sum_{i=1}^n a_{i2}} & \frac{a_{13}}{\sum_{i=1}^n a_{i3}} & \dots & \frac{a_{1n}}{\sum_{i=1}^n a_{in}} \\ \frac{a_{21}}{\sum_{i=1}^n a_{i1}} & \frac{a_{22}}{\sum_{i=1}^n a_{i2}} & \frac{a_{23}}{\sum_{i=1}^n a_{i3}} & \dots & \frac{a_{2n}}{\sum_{i=1}^n a_{in}} \\ \dots & \dots & \dots & \dots & \dots \\ \frac{a_{n1}}{\sum_{i=1}^n a_{i1}} & \frac{a_{n2}}{\sum_{i=1}^n a_{i2}} & \frac{a_{n3}}{\sum_{i=1}^n a_{i3}} & \dots & \frac{a_{nn}}{\sum_{i=1}^n a_{in}} \end{bmatrix} \quad (40)$$

Relative matrix is written as:

$$W_{ij} = \begin{bmatrix} W_1 \\ W_2 \\ W_3 \\ \dots \\ W_n \end{bmatrix} = \begin{bmatrix} \frac{a_{11}}{\sum_{i=1}^n a_{i1}} & \frac{a_{12}}{\sum_{i=1}^n a_{i2}} & \frac{a_{13}}{\sum_{i=1}^n a_{i3}} & \dots & \frac{a_{1n}}{\sum_{i=1}^n a_{in}} \\ \frac{a_{21}}{\sum_{i=1}^n a_{i1}} & \frac{a_{22}}{\sum_{i=1}^n a_{i2}} & \frac{a_{23}}{\sum_{i=1}^n a_{i3}} & \dots & \frac{a_{2n}}{\sum_{i=1}^n a_{in}} \\ \dots & \dots & \dots & \dots & \dots \\ \frac{a_{n1}}{\sum_{i=1}^n a_{i1}} & \frac{a_{n2}}{\sum_{i=1}^n a_{i2}} & \frac{a_{n3}}{\sum_{i=1}^n a_{i3}} & \dots & \frac{a_{nn}}{\sum_{i=1}^n a_{in}} \end{bmatrix} \times \frac{1}{n} \quad (41)$$

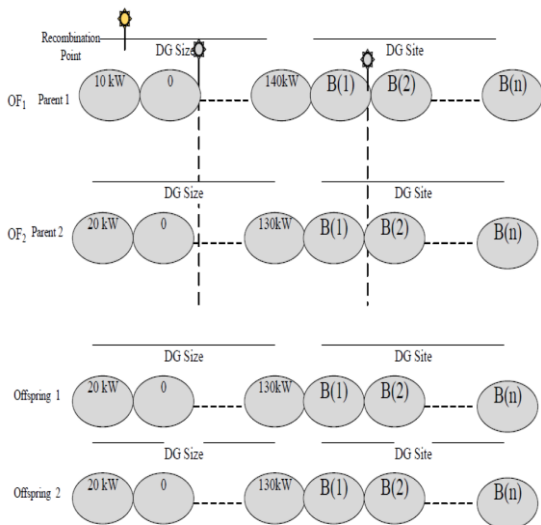


Figure 5. Crossover and mutation process

Eigenvalue matrix is formed as :

$$N_{ij} = \begin{bmatrix} \frac{V_1}{W_1} \\ \frac{V_2}{W_2} \\ \dots \\ \frac{V_n}{W_n} \end{bmatrix} \quad (42)$$

Matrix V_i is formed as :

$$V_i = \begin{bmatrix} \frac{V_1}{W_1} \\ \frac{V_2}{W_2} \\ \dots \\ \frac{V_n}{W_n} \end{bmatrix} = \begin{bmatrix} \frac{a_{11}}{W_1} + \frac{a_{12}}{W_2} + \dots + \frac{a_{1n}}{W_n} \\ \frac{a_{21}}{W_1} + \frac{a_{22}}{W_2} + \dots + \frac{a_{2n}}{W_n} \\ \dots \\ \frac{a_{n1}}{W_1} + \frac{a_{n2}}{W_2} + \dots + \frac{a_{nn}}{W_n} \end{bmatrix} \quad (43)$$

Evaluation matrix is formed as :

$$E_{ij} = \begin{bmatrix} \frac{a_{11}}{W_1} & \frac{a_{12}}{W_2} & \frac{a_{13}}{W_3} & \dots & \frac{a_{1n}}{W_n} \\ \frac{a_{21}}{W_1} & \frac{a_{22}}{W_2} & \frac{a_{23}}{W_3} & \dots & \frac{a_{2n}}{W_n} \\ \dots & \dots & \dots & \dots & \dots \\ \frac{a_{n1}}{W_1} & \frac{a_{n2}}{W_2} & \frac{a_{n3}}{W_3} & \dots & \frac{a_{nn}}{W_n} \end{bmatrix} \quad (44)$$

Maximum eigenvalue is achieved as :

$$\tau_{max} = \left[\frac{V_1}{W_1} + \frac{V_2}{W_2} + \dots + \frac{V_n}{W_n} \right] \times \frac{1}{n} \quad (45)$$

Consistency index is obtained as :

$$CI = \left[\frac{\tau_{max} - n}{n - 1} \right] \times \frac{1}{n} \quad (46)$$

n is number of criteria. Consistency ratio is achieved as :

$$CR = \frac{CI}{RI} \quad (46)$$

RI is random index.

3. RESULTS

In this section all of simulation results are studied in details. Several kinds of technical constraints are considered in the benefit functions. with appropriation the different weights to each function, impacts of technical constraints in total benefits are evaluated. To make a comprehensive analyze, four various scenarios are improvised as follows:

- Scenario 1: Base plan represents the basic structure of the test cases without any WTs
- Scenario 2: Optimal placement of only 1 WT
- Scenario 3: Optimal placement of 2 WTs
- Scenario 4: Optimal placement of 3 WTs

For scenarios 2, 3 and 4 two different states are devised as follows:

- Case-I: Placing WTs operated in unity power factor (UPF)
- Case-II: Placing WTs operated in APF mode

3. 1. Input Data In this paper, 33 bus IEEE system is selected as benchmark system. Figure 6 shows the presented DN by considering three kinds of residential, commercial and industrial loads (31). Total active and reactive power of the mentioned system are 3.72MW and 2.3MVar, respectively. According to the system power, maximum and minimum installing size of DGs are 50% system loads and 200kW, respectively.

Table 1 gives the residential, industrial and commercial loads features. In Table 2, price of exchanging energy has been given. In Table 3, planning parameters are given.

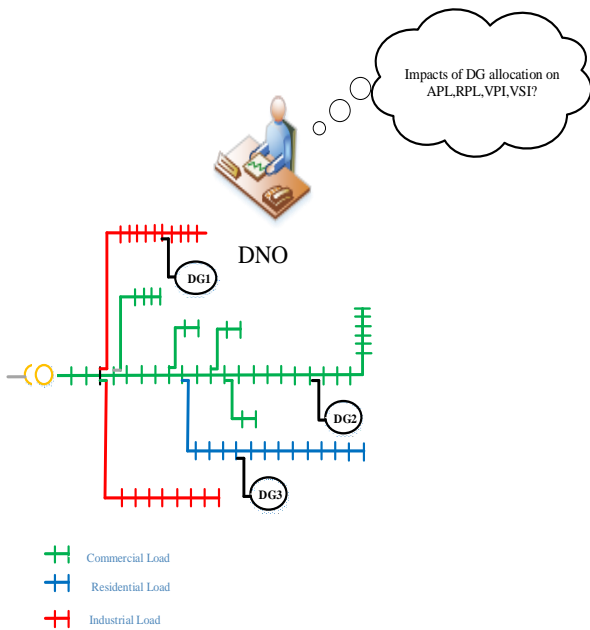


Figure 6. The presented DN

TABLE 1. Parameters of voltage sensitivity of loads

Load model	Dependency coefficient	
	k_{pv}	k_{qv}
Constant	0	0
Residential	1.5	2.4
Industrial	0.2	0.7
Commercial	0.5	2.4

TABLE 2. Price of sold/purchase power

Parameter	Value	Unit
$\rho_{t,h}$	75	\$/MWh
$\rho_{t,h}^{grta}$	65	\$/MWh
C_d	0.001	\$/MWh
IC_b	1000	\$/MWh

TABLE 3. Parameters of planning problem

Parameter	Value	Unit
α	3	%
V_{min}	0.9	p.u
V_{max}	1.1	p.u
InFR	4	%
InTR	5	%
$\sigma_{t,h}$	$0.1 \times \mu_{i,k}$	--

3. 2. Optimal Siting and Sizing of WTs with Considering APL as a Main Technical Constraint

In the presented 33 bus system, feeder 1 is considered as reference bus. Due to budget limitation for operators, three WT with size in [0.2, 20] MW and PF between [0.8,1] p.u are considered in the allocation problem.

As it is given in Table 4, the minimum voltage and active power loss in the base mode is in the bus 18 equal to 0.9038 p.u and 210.98 kW, respectively. Figures (7-9), show the voltage profile for scenarios 2, 3, 4 in mode, respectively. As it can be seen clearly from Figure 8, installing WT with site and size 1.942 MW in bus 8, improve the minimum voltage of bus 18 from 0.91 to 0.948 p.u . Figure 7, illustrates the positive role of installing WT with sizes, 0.857 and 1.204 MW in the buses 13 and 30, in improving the minimum voltage from 0.91 to 0.991. Installing the WTs with sizes 0.749, 0.879 and 0.408 in the buses 14, 25 and 30 improve the voltage profile of buses as Figure 8. In Figure 10 power loss in several scenarios is figured.

Figures 11-13, show the voltage profile for the scenarios 2, 3, 4 in mode 2, respectively. Installing WT (1.911 MW) with the tuned power factor (0.87) improve the voltage profile as Figure 12. Figures 11-13, show the voltage profile for the scenarios 2,3,4 in mode 2, respectively. Installing WT (1.911 MW) with the tuned power factor (0.87) improve the voltage profile as Figure 12. Figure 13 shows the improved voltage profile with installing WT with the size (1.204 MW and 0.857) and tuned power factor (0.9 and 0.87). Equipping DN with three WTs (0.749, 0.879 and 0.408) with tuned power factor in (0.88, 0.92,0.89) improve the buses voltage profile as Figure 14. In Figures 15-16, impacts of increasing the number of WTs on the voltage profile are figured. In Figures 16 and 17, by installing WTs, the voltage magnitude of some buses are more than 1p.u.

In Figures 15-16, impacts of increasing the number of WTs on the voltage profile are figured. In Figures 16 and 17, by installing WTs, the voltage magnitude of some buses are more than 1p.u.

3. 3. Optimal Siting and Sizing of WTs with Considering VSI as a Main Technical Constraint

Table 5 gives the results in the conditions which VSI is

considered as main technical constraints. As it can be seen, different scenarios and modes are considered to have a comprehensive study. Results show the positive impacts of injecting reactive power in the adjustable power factor condition, on reducing active power loss and voltage drop. For example, by comparing different modes of scenario 2, the truth of improving voltage domain with 1 WT in the adjustable power factor with injecting reactive power is cleared.

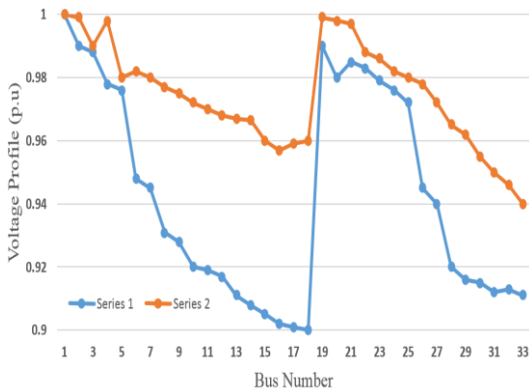


Figure 7. Voltage profile in scenario 2

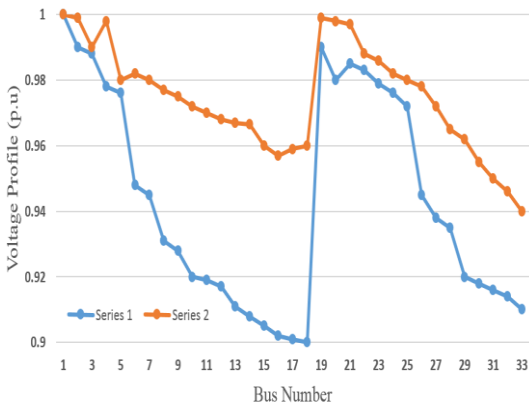


Figure 8. Voltage profile in scenario 3

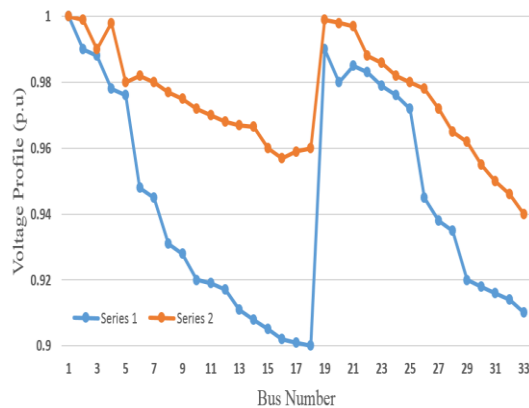


Figure 9. Voltage profile in scenario 4

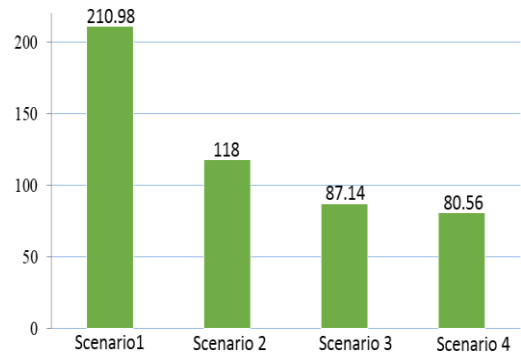


Figure 10. Power loss of each scenario

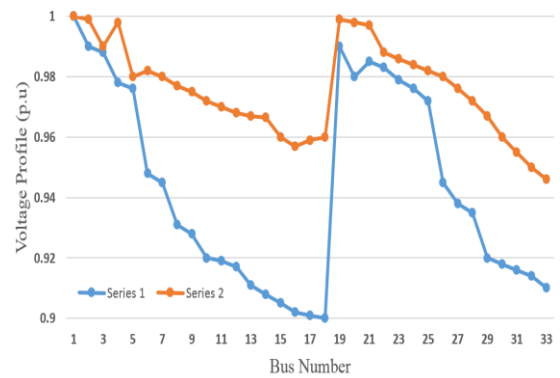


Figure 11. Voltage profile in scenario 2 mode 2

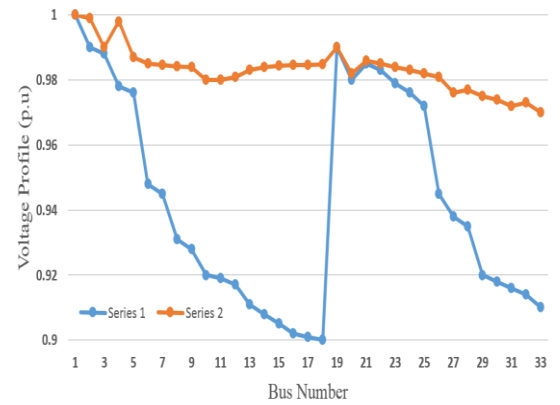


Figure 12. Voltage profile in scenario 3 mode 2

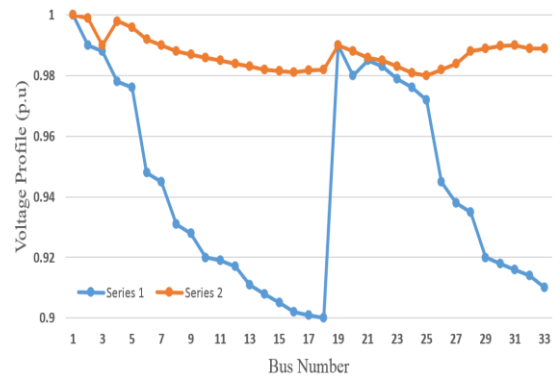


Figure 13. Voltage profile in scenario 4 mode 2

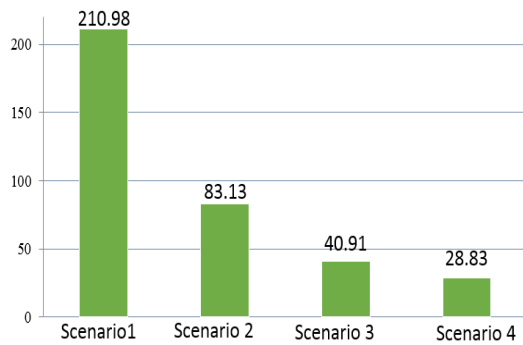


Figure 14. Active power loss in mode 2 (power loss of each scenario)

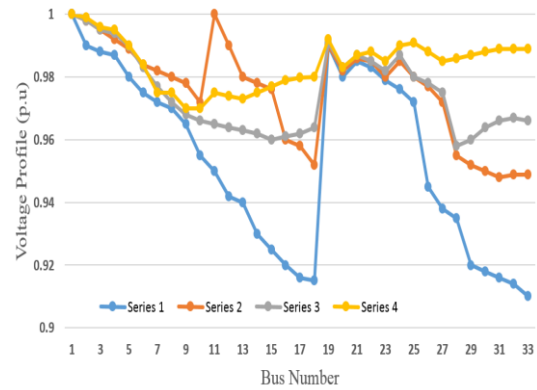


Figure 16. Voltage profile with 1,2,3,4 WT in mode 2

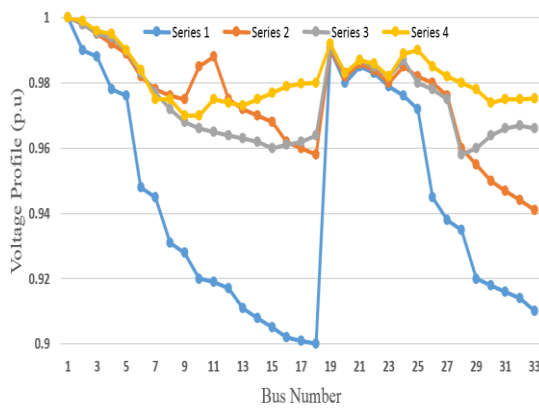


Figure 15. Voltage profile with 1-4 WT in mode 1

3. 4. Optimal Siting and Sizing of WTs with Considering LFL as a Main Technical Constraint

In this section optimal configuration of the WTs by solving benefit functions are done with considering LFL as a main technical constraint. Table 6 gives the obtained results.

Amount of achieved benefit functions are given in Table 7. As it is seen clearly, total achieved benefits by considering active power loss as a main technical constraint is more than others.

3. 5. Employing AHP Figure 17 illustrates the AHP technique to choose the best solution among the obtained solutions of several scenarios. By considering each of functions as a main technical constraint, all of plans and indices are given in Table 8. After employing AHP, the chosen plans for each of functions are plan 3, plan 2 and plan 5, respectively.

3. 6. Evaluating the Proposed VSI in the 118 Bus IEEE System

The IEEE 118 Bus Test Case represents a portion of the American Electric Power System (in the Midwestern US) (32) as shown in Figure 18. By employing the proposed VSI to this system, the minimum value is obtained 0.9521 p.u. Optimal site and size of WTs are obtained buses 12 and 110 with size 0.875 and 1.29 MW, respectively.

TABLE 4. Optimal results with considering active power loss as a main technical constraint

Senario	Mode	Active Power	Active Power Loss Reduction	Minimum Voltage (p.u)	Optimum Siting and Sizing of WT (MW)	Optimum Power factor
1	Base mode	210.98	-	0.918(B18)	-	-
2	Mode 1	118	44.07	0.9038 (B18)	1.942(B8)	1.00
	Mode 2	83.13	60.6	0.9562 (B33)	1.941(B8)	0.87 (B8)
3	Mode 1	87.17	58.68	0.9670(B33)	0.857(B13)	1.00 (B13)
					1.204(B30)	1.00 (B30)
	Mode 2	40.91	80.6	0.9725(B33)	0.871(B16)	0.87 (B16)
4	Mode 1	80.66	61.77	0.9812 (B25)	0.811(B14)	1.00 (B25)
	Mode 2	28.83	86.33	0.96745 (B18)	0.749(B14)	0.88 (B14)
					0.408(B30)	0.89 (B31)

TABLE 5. Optimal results with considering VSI as a main technical constraint

Senario	Mode	Active Power	Active Power Loss Reduction	Minimum Voltage (p.u)	Optimum Siting and Sizing of WT (MW)	Optimum Power factor
1	Base mode	210.98	-	0.918 (B18)	-	-
2	Mode 1	118	44.07	0.9038 (B18)	1.911 (B8)	1.00
	Mode 2	83.13	60.6	0.9562 (B33)	1.912 (B8)	0.86 (B8)
3	Mode 1	87.17	58.68	0.9670 (B33)	0.849 (B13)	1.00 (B13)
					1.151 (B30)	1.00 (B30)
	Mode 2	40.91	80.6	0.9725 (B33)	0.86 (B16)	0.85 (B16)
4	Mode 1	80.66	61.77	0.9812 (B25)	1.134 (B30)	0.9 (B30)
					0.728 (B14)	1.00 (B14)
					1.00 (B25)	1.00 (B25)
	Mode 2	28.83	86.33	0.96745 (B18)	0.733 (B14)	0.86 (B14)
					0.847 (B25)	0.9 (B25)
					0.378 (B30)	0.86 (B31)

TABLE 6. Optimal results with considering LFL as a main technical constraint

Senario	Mode	Active Power	Active Power Loss Reduction	Minimum Voltage (p.u)	Optimum Siting and Sizing of WT (MW)	Optimum Power factor
1	Base mode	210.98	-	0.9038 (B18)	-	-
2	Mode 1	112	46.67	0.9472 (B33)	1.911 (B8)	1.00
	Mode 2	82.15	60.89	0.9560 (B33)	1.912 (B8)	0.88 (B8)
3	Mode 1	85.41	59.33	0.9643 (B33)	0.849 (B13)	1.00 (B13)
					1.151 (B30)	1.00 (B30)
	Mode 2	39.62	81.13	0.9765 (B25)	0.862 (B16)	0.88 (B16)
4	Mode 1	79.74	62.03	0.95785 (B18)	1.134 (B30)	0.9 (B30)
					0.728 (B14)	1.00 (B14)
					1.00 (B25)	1.00 (B25)
	Mode 2	26.58	87.34	0.9795 (B30)	0.733 (B14)	0.87 (B14)
					0.856 (B25)	0.91 (B25)
					0.421 (B30)	0.88 (B31)

TABLE 7. Achieved benefits of different benefit functions with considering LFL as a main technical constraint

Benefits (*10 ⁷ \$)	Senario			
	1	2	3	4
The benefit of reducing dependency on upstream grid	1.015	1.023	1.038	1.075
The benefits of reducing reactive power loss	1.101	1.108	1.109	1.208
The benefit of reducing power loss	1.428	1.475	1.502	1.678
The benefit of improving voltage stability	1.243	1.305	1.375	1.457
Total benefit (\$)	1.578	1.605	1.642	1.708

4. DISCUSSIONS

In this section the performance of the proposed VSI with two other VSIs is compared. Different VSIs are

determined in 33, 67 and 118 buses IEEE radial distribution system. As it seen from Table 9, the proposed VSI has an efficient role in the determining WT sizes in the improving voltage profile.

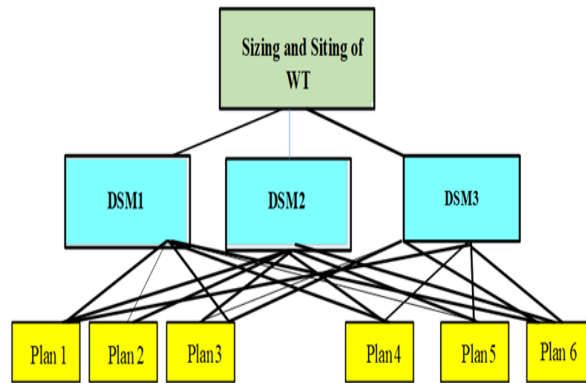


Figure 17. AHP technique with 6 plans

TABLE 8. Alternatives and indices of AHP

OF1= Power Loss Minimization			OF2= Voltage Profile Improvement			OF3= load flow limitation		
$P_{Loss}(x, u) = \sum_k I_k ^2 R_k$			$VSI = \left[1 - \frac{4 \left(\frac{P_2^2 + Q_2}{Q_2} \right) X}{\left(\frac{P_2 \sin \delta V_1}{Q_2} - V_1 \cos \delta \right)^2} \right]$			$LFL = \text{Max} \left(\frac{S_{ij}}{CS_{ij}} \right)$		
Senario	Mode	Plans	Senario	Mode	Plans	Senario	Mode	Plans
2	Case-I	Plan 1	2	Case-I	Plan 7	2	Case-I	Plan 13
	Case-II	Plan 2		Case-II	Plan 8		Case-II	Plan 14
3	Case-I	Plan 3	3	Case-I	Plan 9	3	Case-I	Plan 15
	Case-II	Plan 4		Case-II	Plan 10		Case-II	Plan 16
4	Case-I	Plan 5	4	Case-I	Plan 11	4	Case-I	Plan 17
	Case-II	Plan 6		Case-II	Plan 12		Case-II	Plan 18

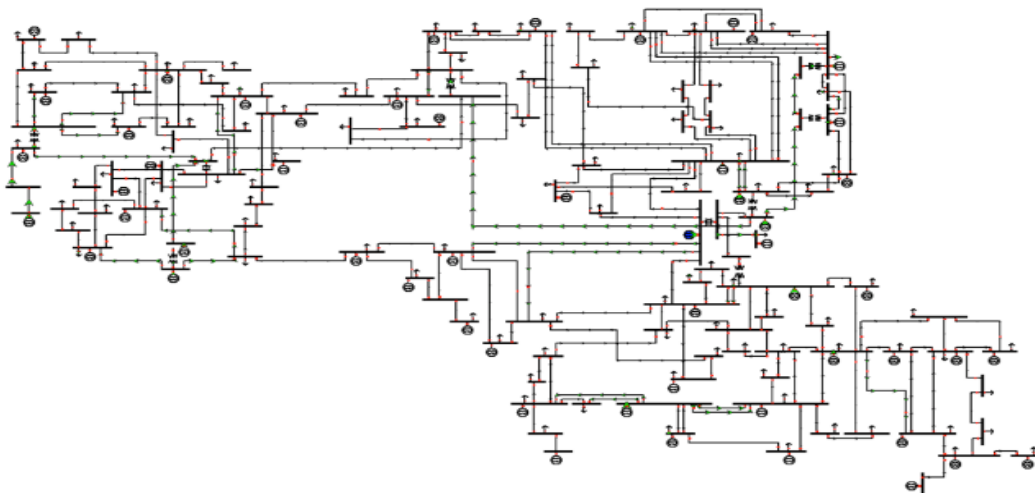


Figure 18. IEEE118 bus test system

Impacts of new VSI performance in improving voltage profile of constant, residential, commercial and industrial loads are shown in Figures 19-22.

It's obviously seen, presence of WT improve the value of nod's VSI in compared with base mode in the several types of load (commercial, industrial and

TABLE 9. Comparing different VSI with the proposed index

VSI	33 Bus	67 Bus	118 Bus
The proposed index	0.9725	0.9642	0.9521
$V_{Bus-min} = \max(1 - V_n)$	0.9652	114.3	95.9
$VSI_{(m2)} = V_{(m1)} ^4 - 4\{P_{(m2)} \times (jj) - Q_{(m2)}r(jj)^2\} - 4\{P_{(m2)} \times r(jj) + Q_{(m2)} \times (jj)\} V_{(m1)} ^2$	0.9672	0.9601	0.9514
$LVSI = \frac{4RP_r}{V_2 \cos\theta - \delta \leq 1}$	0.9651	0.9589	0.9510
$LVSI = \frac{4(Vi Vj \cos\delta - Vj^2 \cos\delta^2)}{Vi^2}$	0.9430	0.9521	0.9641
$LVSI = \sqrt{\frac{V_i^2 - 2Z(Pr \cos\theta + Qr \sin\theta)}{2}}$	0.9285	0.9486	0.9514

residential). The value of minimum VSI in the industrial load is 1.01 in the bus 18 and that corresponding to the absence of WT is 0.8081. in the constant, residential and commercial loads, this value is determined, 1.015, 1.018 and 1.017, respectively.

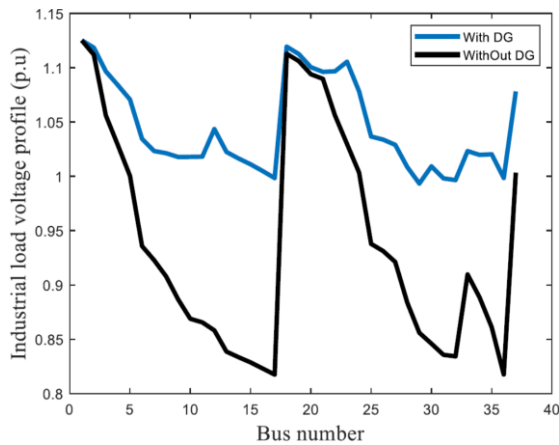


Figure 19. Impacts of the new VSI in improving voltage profile of Industrial load

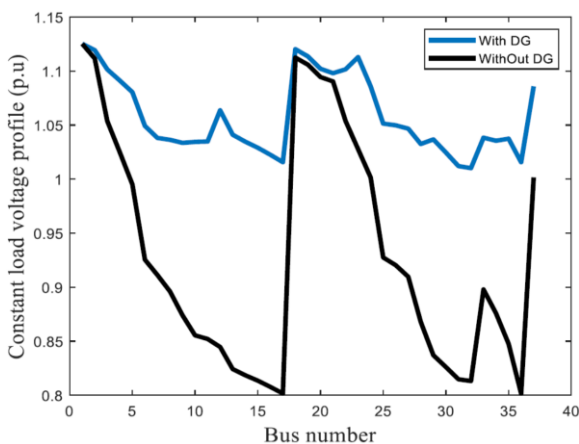


Figure 20. Impacts of the new VSI in improving voltage profile of constant load

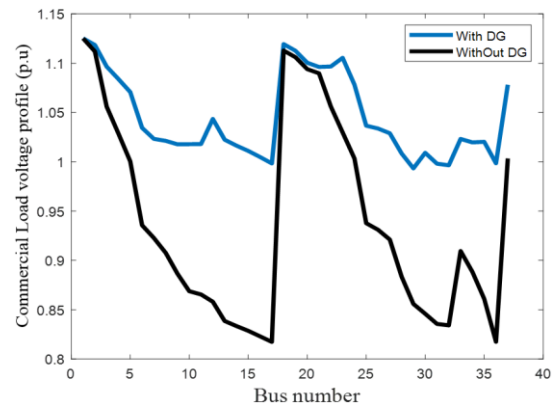


Figure 21. Impacts of the new VSI in improving voltage profile of commercial load

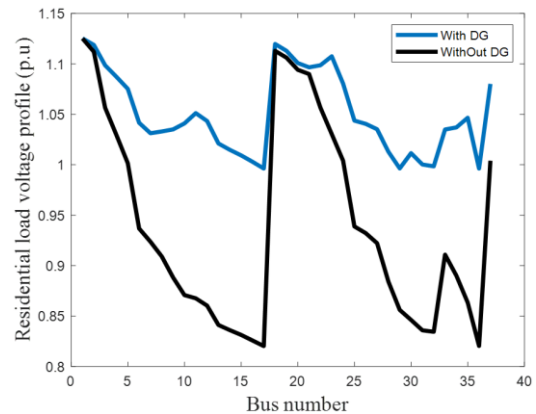


Figure 22. Impacts of the new VSI in improving voltage profile of residential load

5. CONCLUSION

In this paper new approach is introduced to calculate the voltage stability index under installing WT and in various operational conditions. Besides VSI, active and reactive power loss and voltage profile indices are used as technical constraints. Three main functions, which

include the positive effects of the presence of WT in improving technical constraints and maximizing benefits of the demand side, are defined as objective functions. By multiplying each function in the specified weight and assigning the weight with a high value to the critical technical constraint, the total benefit function is formed. Due to planning problem with the multi-criteria essence, the obtained results of the genetic algorithm (GA) are arranged by applying the AHP technique. Various scenarios are solved in two modes, unified and adjusted power factors. Results verified the efficiency and performance of the proposed GA-AHP optimization algorithm.

6. REFERENCES

- Farzinfar M, Jazaeri M. A novel methodology in optimal setting of directional fault current limiter and protection of the MG. *International Journal of Electrical Power & Energy Systems*. 2020;116:105564. 10.1016/j.ijepes.2019.105564
- Sundarajoo S, Soomro DM. Optimal Load Shedding for Voltage Collapse Prevention Following Overloads in Distribution System. *International Journal of Engineering, Transactions A: Basics*. 2023;36(7):1230-8. 10.5829/IJE.2023.36.07A.04
- Mobashsher MM, Keypour R, Savaghebi M. Distributed optimal voltage control in islanded microgrids. *International Transactions on Electrical Energy Systems*. 2021;31(11):e13045. 10.1002/2050-7038.13045
- Tooryan F, HassanzadehFard H, Collins ER, Jin S, Ramezani B. Optimization and energy management of distributed energy resources for a hybrid residential microgrid. *Journal of Energy Storage*. 2020;30:101556. 10.1016/j.est.2020.101556
- Yousefipour A, Rahmani A, Jahanshahi M. Improving the load balancing and dynamic placement of virtual machines in cloud computing using particle swarm optimization algorithm. *International Journal of Engineering, Transactions C: Aspects*. 2021;34(6):1419-29. 10.5829/IJE.2021.34.06C.05
- Wang G, Wang Q, Qiao Z, Wang J, Anderson S. Optimal planning of multi-micro grids based-on networks reliability. *Energy Reports*. 2020;6:1233-49. 10.1016/j.egy.2020.05.007
- Elmaadawy K, Kotb KM, Elkadeem M, Sharshir SW, Dán A, Moawad A, et al. Optimal sizing and techno-enviro-economic feasibility assessment of large-scale reverse osmosis desalination powered with hybrid renewable energy sources. *Energy Conversion and Management*. 2020;224:113377. 10.1016/j.enconman.2020.113377
- Mubaarak S, Zhang D, Wang L, Mohan M, Kumar PM, Li C, et al. Efficient photovoltaics-integrated hydrogen fuel cell-based hybrid system: Energy management and optimal configuration. *Journal of Renewable and Sustainable Energy*. 2021;13(1). 10.1063/1.5141932
- Mehranfar N, Hajiaghaei-Keshteli M, Fathollahi-Fard AM. A novel hybrid whale optimization algorithm to solve a production-distribution network problem considering carbon emissions. *International Journal of Engineering, Transactions C: Aspects*. 2019;32(12):1781-9. 10.5829/IJE.2019.32.12C.11
- Bujal NR, Sulaiman M, Abd Kadir AF, Khatib T, Eltawil N. A Comparison between GSA and IGSA for optimal allocation and sizing of dg and impact to voltage stability margin in electrical distribution system. *Journal of Electrical Engineering & Technology*. 2021;16:2949-66. 10.1007/s42835-021-00829-y
- Mastoi MS, Tahir M, Usman M, Wang D, Zhuang S, Hassan M. Research on power system transient stability with wind generation integration under fault condition to achieve economic benefits. *IET Power Electronics*. 2022;15(3):263-74. 10.1049/pe12.12228
- Azad S, Amiri MM, Heris MN, Mosallanejad A, Ameli MT. A novel analytical approach for optimal placement and sizing of distributed generations in radial electrical energy distribution systems. *Sustainability*. 2021;13(18):10224. 10.3390/su131810224
- Mirjalili S, Gandomi AH, Mirjalili SZ, Saremi S, Faris H, Mirjalili SM. Salp Swarm Algorithm: A bio-inspired optimizer for engineering design problems. *Advances in engineering software*. 2017;114:163-91. 10.1016/j.advengsoft.2017.07.002
- Barnwal AK, Yadav LK, Verma MK. A multi-objective approach for voltage stability enhancement and loss reduction under PQV and P buses through reconfiguration and distributed generation allocation. *IEEE Access*. 2022;10:16609-23. 10.1109/ACCESS.2022.3146333
- Nageswari D, Kalaiarasi N, Geethamahalakshmi G. Optimal Placement and Sizing of Distributed Generation Using Metaheuristic Algorithm. *Comput Syst Sci Eng*. 2022;41(2):493-509. 10.32604/csse.2022.020539
- Nafeh AA, Heikal A, El-Sehiemy RA, Salem WA. Intelligent fuzzy-based controllers for voltage stability enhancement of AC-DC micro-grid with D-STATCOM. *Alexandria Engineering Journal*. 2022;61(3):2260-93. 10.1016/j.aej.2021.07.012
- Onlam A, Yodphet D, Chatthaworn R, Surawanitkun C, Siritaratiwat A, Khunkitti P. Power loss minimization and voltage stability improvement in electrical distribution system via network reconfiguration and distributed generation placement using novel adaptive shuffled frogs leaping algorithm. *Energies*. 2019;12(3):553. 10.3390/en12030553
- Hamid ZA, Jipinus S, Musirin I, Othman MM, Salimin RH. Optimal sizing of distributed generation using firefly algorithm and loss sensitivity for voltage stability improvement. *Indonesian Journal of Electrical Engineering and Computer Science*. 2020;17(2):720-7. 10.11591/ijeecs.v17.i2.pp720-727
- Mehta P, Bhatt P, Pandya V. Optimal selection of distributed generating units and its placement for voltage stability enhancement and energy loss minimization. *Ain Shams Engineering Journal*. 2018;9(2):187-201. 10.1016/j.asej.2015.10.009
- Ahangar ARH, Gharehpetian GB, Baghaee HR. A review on intentional controlled islanding in smart power systems and generalized framework for ICI in microgrids. *International Journal of Electrical Power & Energy Systems*. 2020;118:105709. 10.1016/j.ijepes.2019.105709
- Guerrero JM, Loh PC, Lee T-L, Chandorkar M. Advanced control architectures for intelligent microgrids—Part II: Power quality, energy storage, and AC/DC microgrids. *IEEE Transactions on industrial electronics*. 2012;60(4):1263-70. 10.1109/TIE.2012.2196889
- Sundarajoo S, Soomro DM. Optimal Load Shedding for Voltage Collapse Prevention Following Overloads in Distribution System. *International Journal of Engineering*. 2023;36(7):1230-8. 10.5829/IJE.2023.36.07A.04
- Sadeghi SE, Akbari Foroud A. A general index for voltage stability assessment of power system. *International Transactions on Electrical Energy Systems*. 2021;31(12):e13155. doi.org/10.1002/2050-7038.13155
- Sadeghi SE, Akbari Foroud A. A new approach for static voltage stability assessment in distribution networks. *International Transactions on Electrical Energy Systems*. 2020;30(3):e12203. doi.org/10.1002/2050-7038.12203

25. Bai W, Abedi MR, Lee KY. Distributed generation system control strategies with PV and fuel cell in microgrid operation. *Control Engineering Practice*. 2016;53:184-93. 10.1016/j.conengprac.2016.02.002
26. Samadi A, Eriksson R, Söder L, Rawn BG, Boemer JC. Coordinated active power-dependent voltage regulation in distribution grids with PV systems. *IEEE Transactions on power delivery*. 2014;29(3):1454-64. 10.1109/TPWRD.2014.2298614
27. Jia H, Hou Q, Yong P, Liu Y, Zhang N, Liu D, et al. Voltage stability constrained operation optimization: An ensemble sparse oblique regression tree method. *IEEE Transactions on Power Systems*. 2023. <https://doi.org/10.1109/TPWRS.2023.3236164>
28. Kyomugisha R, Muriithi CM, Nyakoe GN. Performance of various voltage stability indices in a stochastic multiobjective optimal power flow using mayfly algorithm. *Journal of Electrical and Computer Engineering*. 2022;2022. 10.1155/2022/7456333
29. Mahmoud MM, Esmail YM, Atia BS, Kamel OM, AboRas KM, Bajaj M, et al. Voltage quality enhancement of low-voltage smart distribution system using robust and optimized DVR controllers: Application of the Harris hawks algorithm. *International Transactions on Electrical Energy Systems*. 2022;2022. 10.1155/2022/4242996
30. Li B, Hu K, Ma J, Xu S, He Y, Jiao H, et al. The new definitions of loss function for the model-based parameter identification method in power distribution network. *International Transactions on Electrical Energy Systems*. 2022;2022. 10.1155/2022/4197043
31. Hossen MD, Islam MF, Ishraque MF, Shezan SA, Arifuzzaman S. Design and implementation of a hybrid solar-wind-biomass renewable energy system considering meteorological conditions with the power system performances. *International journal of photoenergy*. 2022;2022. 10.1155/2022/8792732
32. Gupta SK. Mathematical Modeling and Analysis of Improved Grey Wolf Optimization Algorithm-Based Multi-Objective Power Flow Optimization for IEEE-118 Bus Test System. *Rivista Italiana di Filosofia Analitica Junior*. 2023;14(2):395-408. 10.52783/tjpt.v44.i2.139

COPYRIGHTS

©2024 The author(s). This is an open access article distributed under the terms of the Creative Commons Attribution (CC BY 4.0), which permits unrestricted use, distribution, and reproduction in any medium, as long as the original authors and source are cited. No permission is required from the authors or the publishers.



Persian Abstract

چکیده

به طور کلی یک شبکه توزیع از ژنراتورها و زیرساخت‌های ارتباطی تشکیل می‌شود. امروزه با توجه به افزایش تقاضای بار و همچنین رشد تولیدات پراکنده، استفاده از این نوع ژنراتورها در شبکه توزیع شدت گرفته است. در مناطقی که سرعت وزش باد مناسب وجود داشته باشد، استفاده از توربین‌های بادی به عنوان یک گام هوشمند در شبکه توزیع تلقی می‌گردد. پایداری ولتاژ همواره به عنوان یک شاخصه اصلی جهت پایداری شبکه و پاسخ‌گویی به نیازهای مصرف‌کننده شناخته شده است. تاکنون شاخص‌های متعددی جهت ارزیابی پایداری ولتاژ معرفی شده است، با این حال هیچ کدام از این شاخص‌ها جواب بهینه‌ای ارائه نکرده‌اند. شاخص ارائه شده در این مقاله تلفات توان اکتیو، راکتیو و پایداری ولتاژ را به عنوان محدودیت‌های فنی مسئله بهینه‌سازی در خود جای داده است. به منظور بررسی تاثیر حضور توربین‌های بادی، مسئله بهینه‌سازی در دو حالت ضریب توان بار واحد و ضریب توان بار تلفیقی با بارهای خطی بررسی شده است. برای حل مسئله بهینه‌سازی از الگوریتم ژنتیک استفاده شده است و با استفاده از تکنیک AHP و در نظر گرفتن هر یک از محدودیت‌های فنی به عنوان معیار اصلی، جواب‌های به دست آمده مرتب می‌شوند. برای تأیید اثربخشی مثبت شاخص پیشنهادی، نتایج آن با نتایج سایر شاخص‌ها در شبکه توزیع شعاعی استاندارد 33-67 و 118 باس IEEE مقایسه شده است.